INTERNATIONAL JOURNAL FOR NUMERICAL METHODS IN FLUIDS
Int. J. Numer. Meth. Fluids 2006; **51**:425–438
Published online 6 December 2005 in Wiley InterScience (www.interscience.wiley.com). DOI: 10.1002/fld.1139

Magnetic effect on the formation of longitudinal vortices in a rotating laminar boundary layer

Ming-Han Lin*,†

Department of Automation Engineering, Ta-Hwa Institute of Technology, Hsinchu 307, Taiwan, ROC

SUMMARY

This paper presents a numerical study of magnetic effect on the formation of longitudinal vortices in a rotating laminar boundary layer. The criterion for the position marking the onset of longitudinal vortices is defined in this paper. The onset position characterized by the rotational Goertler number $G_{\delta,\mathrm{rot}}$, depends on the local rotation number, Reynolds number, the magnetic field parameter, the Prandtl number and the wave number. The results show that positive rotation destabilizes the flow. The flow is found to become more unstable to the vortex mode of instability as the value of magnetic field parameter M increases. The numerical data shows good agreement with the experimental results. Copyright © 2005 John Wiley & Sons, Ltd.

KEY WORDS: vortex instability; rotation; longitudinal vortices; magnetic effect

INTRODUCTION

A Blasius boundary layer flow over a horizontal plate with rotation has received considerable attention in the past few decades. The study of vortex instability in a laminar boundary layer with the effect of rotation is of practical significance for its engineering applications. With the development of turbomachinery, the study of flow instabilities in rotating laminar boundary layers has recently become an important research area. Meanwhile, the study of magnetohydrodynamics plays an important role in engineering industries. The problem of a Blasius boundary layer flow under the influence of a magnetic field also has many applications in geophysics and astrophysics.

*Correspondence to: Ming-Han Lin, Department of Automation Engineering, Ta-Hwa Institute of Technology, Hsinchu 307, Taiwan, ROC.
†E-mail: aemhlin@thit.edu.tw

Contract/grant sponsor: National Science Council; contract/grant number: NSC 93-2212-E-233-002

Received 1 July 2005
Revised 12 October 2005
Accepted 20 October 2005

There are some literature on the vortex instability in a Blasius boundary layer over a horizontal plate with rotation (for example, References Conrad [1], Chawla [2], Koyama *et al.* [3], Masuda *et al.* [4], Matubara and Masuda [5], Lin and Hwang [6], etc.). Recently, the experimental and numerical methods employed in the literature for onset of longitudinal vortices were summarized in Reference Hwang and Lin [7]. It is noted that magnetic effect on the onset of longitudinal vortices of a Blasius boundary layer flow with rotation has engineering application in electrical machinery cooling. This topic is not yet completely elucidated in published bibliography and that will be analysed in this paper. We propose in this paper to study the problem of magnetic effect on the onset and subsequent linear development of longitudinal vortices of a Blasius boundary layer flow with rotation. The experimental criteria proposed by Hwang and Lin [7] on the onset of longitudinal vortices were employed in the present study. The governing parameters on the onset of longitudinal vortices are the Prandtl number, the wave number a, the magnetic field parameter M, the Reynolds number, and the local rotation number. In the computation, the magnitudes of applied initial perturbation velocity with an amplitude of $u^0 = 10^{-4}$ is employed.

THEORETICAL ANALYSIS

A laminar Blasius flow is chosen as a basic flow. Free stream velocity is U_∞ over a flat plate rotating at a positive constant angular speed along an axis accordant with the plate spanwise direction. The flow of the electrically conducting fluid is considered as viscous incompressible, and under the influence of uniform vertical applied magnetic field, as shown in Figure 1. The applied uniform magnetic filed is B_0. It is assumed that the interaction within the flow of the induced magnetic field is negligible when compared with the influence of the applied magnetic field with the flow. In addition, there is no applied electric field and the Hall effect, Joule heating and viscous dissipation are all neglected. The physical coordinates are chosen such that X measures the streamwise distance from the leading edge of the plate, Y is the distance normal to the plate, and Z is in the transverse direction. The present study assumes constant fluid thermophysical properties. The streamwise and normal velocity components of the basic flow are U_b and V_b. The governing boundary layer equations for constant-property fluids, under the Boussinesq approximation and for large Reynolds numbers, can be written as (Singh *et al.* [8])

$$\frac{\partial U_\mathrm{b}}{\partial X} + \frac{\partial V_\mathrm{b}}{\partial Y} = 0 \tag{1}$$

$$U_\mathrm{b}\frac{\partial U_\mathrm{b}}{\partial X} + V_\mathrm{b}\frac{\partial U_\mathrm{b}}{\partial Y} = \mu\frac{\partial^2 U_\mathrm{b}}{\partial Y^2} - \frac{\sigma B_0^2}{\rho}U_\mathrm{b} \tag{2}$$

$$U_\mathrm{b}\frac{\partial T_\mathrm{b}}{\partial X} + V_\mathrm{b}\frac{\partial T_\mathrm{b}}{\partial Y} = \alpha\frac{\partial^2 T_\mathrm{b}}{\partial Y^2} \tag{3}$$

The pressure gradient $\partial p/\partial X$ is neglected due to order of magnitude analysis and assumption of boundary layer flow along a flat plate, as shown in many text books. Next, one introduces

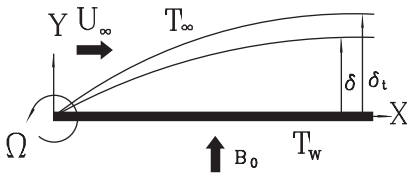

Figure 1. Physical configuration and coordinate system in a rotating boundary layer under the influence of a magnetic field.

the following dimensionless variables and parameters:

$$
\begin{aligned}
&X = Lx, \quad Y = L\,Re_L^{-1/2} y \\
&U_\mathrm{b} = U_\infty \bar{u}, \quad V_\mathrm{b} = U_\infty\, Re_L^{-1/2} \bar{v}, \quad \theta_\mathrm{b} = \frac{T_\mathrm{b} - T_\infty}{T_w - T_\infty} \\
&\eta = Y(U_\infty/\mu X)^{1/2} = y/\sqrt{x}, \quad f(X,\eta) = \psi/(\mu U_\infty L x)^{1/2} \\
&M = \frac{\sigma B_0^2 L}{\rho U_\infty}, \quad Re_L = \frac{U_\infty L}{\mu}, \quad U_\mathrm{b} = \frac{\partial \psi}{\partial Y}, \quad V_\mathrm{b} = -\frac{\partial \psi}{\partial X}
\end{aligned}
\tag{4}
$$

where $f(X,\eta)$ is the reduced stream function, T_w is the surface temperature, and T_∞ is the free-stream temperature.

The free-stream condition should be modified because of non-zero relative vorticity in the free stream. For this reason, the Blasius profile is modified by simply adding $2\Omega Y$ (Matubara and Masuda [9], and Chen and Lin [10]). i.e.

$$
\begin{aligned}
&\bar{U} = \bar{U}_\mathrm{b} + 2\Omega Y \quad \text{(dimensional form) or} \\
&f' = f'_\mathrm{b} + 2\frac{\Omega L}{U_\infty} Re_L^{-1/2} y = f'_\mathrm{b} + 2Ro\, Re_L^{-1/2} \sqrt{x}\eta \quad \text{(dimensionless form)}
\end{aligned}
\tag{5}
$$

Where the basic flow of f_b and θ_b are obtained from the following equations:

$$
f'''_\mathrm{b} + \left(\frac{1}{2} f_\mathrm{b} + x\frac{\partial f_\mathrm{b}}{\partial x}\right) f''_\mathrm{b} - x f'_\mathrm{b} \frac{\partial f'_\mathrm{b}}{\partial x} - xM f'_\mathrm{b} = 0 \tag{6}
$$

$$
\theta''_\mathrm{b} + \left(\frac{1}{2} f_\mathrm{b} + x\frac{\partial f_\mathrm{b}}{\partial x}\right) Pr\, \theta'_\mathrm{b} - x\, Pr\, f'_\mathrm{b} \frac{\partial \theta'_\mathrm{b}}{\partial x} = 0 \tag{7}
$$

The boundary conditions are as follows:

$$
\begin{aligned}
f_\mathrm{b}(x,0) = f'_\mathrm{b}(x,0) = \theta_\mathrm{b}(x,0) - 1 = 0 \\
f'_\mathrm{b}(x,\infty) - 1 = \theta_\mathrm{b}(x,\infty) = 0
\end{aligned}
\tag{8}
$$

In Equations (5)–(7), the primes denote partial derivatives with respect to η and Pr is the Prandtl number.

The standard method of linear stability method is applied with terms higher than first order in disturbance quantities being neglected. The disturbances superimposed on the two-dimensional basic flow quantities can be expressed using complex quantities:

$$\begin{aligned} F(X,Y,Z) &= F_{\mathrm{b}}(X,Y) + \zeta(X,Y)\exp(\mathrm{i}a'Z) = F_{\mathrm{b}}(X,Y) + \zeta(X,Y)\cos(a'Z) \\ W(X,Y,Z) &= w'(X,Y)\mathrm{i}\exp(\mathrm{i}a'Z) = w'(X,Y)\sin(a'Z) \end{aligned} \tag{9}$$

where $F = U, V, P$ or T, $\zeta = u', v', p'$ or t'. The value $a' = 2\pi/\lambda$ is the dimensional transverse wave number of the vortex rolls. By consideration of the vortex-type perturbation quantities in continuity equation, a different expression for W is used.

Substituting Equation (9) into the continuity, Navier–Stokes, and energy equations in 3D Cartesian coordinates, and subtracting the two-dimensional basic flow and energy equations under the assumptions of $Re_L \gg 1$ and $Ro \sim O(1)$, one can obtain the linearized perturbation equations.

$$\frac{\partial u'}{\partial x} + \frac{\partial v'}{\partial y} - a'w' = 0 \tag{10}$$

$$U_{\mathrm{b}}\frac{\partial u'}{\partial X} + u'\frac{\partial U_{\mathrm{b}}}{\partial X} + V_{\mathrm{b}}\frac{\partial u'}{\partial Y} + v'\frac{\partial U_{\mathrm{b}}}{\partial Y} = \mu\nabla^2 u' - \frac{\sigma B_0^2}{\rho}u' + 2\Omega v' \tag{11}$$

$$U_{\mathrm{b}}\frac{\partial v'}{\partial X} + u'\frac{\partial V_{\mathrm{b}}}{\partial X} + V_{\mathrm{b}}\frac{\partial v'}{\partial Y} + v'\frac{\partial V_{\mathrm{b}}}{\partial Y} = \mu\nabla^2 v' - \frac{1}{\rho}\frac{\partial p'}{\partial Y} + 2\Omega u' \tag{12}$$

$$U_{\mathrm{b}}\frac{\partial w'}{\partial X} + V_{\mathrm{b}}\frac{\partial w'}{\partial Y} = \mu\nabla^2 w' - \frac{1}{\rho}\frac{\partial p'}{\partial Z} - \frac{\sigma B_0^2}{\rho}w' \tag{13}$$

$$U_{\mathrm{b}}\frac{\partial t'}{\partial X} + u'\frac{\partial T_{\mathrm{b}}}{\partial X} + V_{\mathrm{b}}\frac{\partial t'}{\partial Y} + v'\frac{\partial T_{\mathrm{b}}}{\partial Y} = \alpha\nabla^2 t' \tag{14}$$

where β is coefficient of thermal expansion, and $\nabla^2 = (\partial^2/\partial Y^2) - a'^2$ is a two-dimensional Laplacian operator. The perturbation equations are two-dimensional and of boundary layer flow type.

Next, one introduces the following dimensionless variables and parameters:

$$\begin{gathered} X = Lx, \quad [Y,Z] = L\,Re_L^{-1/2}[y,z] \\ [U_{\mathrm{b}}, u'] = U_\infty[\bar{u}, u], \quad [V_{\mathrm{b}}, v', w'] = U_\infty\,Re_L^{-1/2}[\bar{v}, v, w] \\ [T_{\mathrm{b}} - T_\infty, t'] = (T_w - T_\infty)[\theta_{\mathrm{b}}, t], \quad p' = \frac{\rho U_\infty^2}{Re_L}p, \quad a' = \frac{Re_L^{1/2}}{L}a \\ Re_L = \frac{U_\infty L}{\mu}, \quad Ro = \frac{\Omega L}{U_\infty}, \quad G_{L,\mathrm{rot}} = 2Ro\,Re_L^{1/2} \end{gathered} \tag{15}$$

and a vorticity function in the axial direction

$$\xi = \frac{\partial w}{\partial y} - \frac{\partial v}{\partial z} = \frac{\partial w}{\partial y} - av \tag{16}$$

To obtain equation for the vorticity, one may differentiate Equations (12) and (13) by z and y, respectively, and then eliminate the pressure terms by subtracting one from the other. To derive the equation for v, one may differentiate Equation (16) with respect to z. Similarly, the equation for w can be obtained by differentiating Equation (16) by y. It is noted that in the derivation of equations for v and w, continuity Equation (10) must be considered. By also using the similarity variable $\eta = y/\sqrt{x}$, the perturbation equations can be transforming from (X, Y) into (x, η) plane.

$$\frac{\partial^2 u}{\partial \eta^2} + \left(\frac{1}{2}f + x\frac{\partial f}{\partial x}\right)\frac{\partial u}{\partial \eta} - xf'\frac{\partial u}{\partial x} - \left(a^2 x + x\frac{\partial f'}{\partial x} - \frac{1}{2}\eta f''\right)u - Mxu = f''\sqrt{x}v \tag{17}$$

$$\frac{\partial^2 t}{\partial \eta^2} + \frac{1}{2}Pr\, f\frac{\partial t}{\partial \eta} - xPr\, f'\frac{\partial t}{\partial x} - a^2 xt = Pr\frac{\partial \theta_b}{\partial \eta}\left(-\frac{1}{2}\eta u + \sqrt{x}v\right) \tag{18}$$

$$\begin{aligned}\frac{\partial^2 \xi}{\partial \eta^2} &+ \left(\frac{1}{2}f + x\frac{\partial f}{\partial x}\right)\frac{\partial \xi}{\partial \eta} - xf'\frac{\partial \xi}{\partial x} - \left(\frac{1}{2}\eta f'' + a^2 x - x\frac{\partial f'}{\partial x}\right)\xi \\ &= -xaG_{L,\mathrm{rot}}u - au\left(\frac{1}{4\sqrt{x}}(f - \eta f' - \eta^2 f'') + \sqrt{x}\left(\eta\frac{\partial f'}{\partial x} - \frac{\partial f}{\partial x}\right) - x^{3/2}\frac{\partial^2 f}{\partial x^2}\right) \\ &+ \sqrt{x}f''\left(\frac{\partial w}{\partial x} - \frac{\eta}{2x}\frac{\partial w}{\partial \eta}\right) + M\sqrt{x}\frac{\partial w}{\partial \eta}\end{aligned} \tag{19}$$

$$\frac{\partial^2 v}{\partial \eta^2} - xa^2 v = axv - \sqrt{x}\frac{\partial^2 u}{\partial x \partial \eta} + \frac{\eta}{2\sqrt{x}}\frac{\partial^2 u}{\partial \eta^2} + \frac{1}{2\sqrt{x}}\frac{\partial u}{\partial \eta} \tag{20}$$

$$\frac{\partial^2 w}{\partial \eta^2} - xa^2 w = \sqrt{x}\frac{\partial \xi}{\partial \eta} - ax\frac{\partial u}{\partial x} + \frac{1}{2}a\eta\frac{\partial u}{\partial \eta} \tag{21}$$

The above equations are in x–η plane instead of x–y plane. The set of Equations (17)–(21) is a boundary value problem in η direction, an initial value problem in x direction, and an eigenvalue problem in z direction. The appropriate initial and boundary conditions for the perturbations equations are

$$\begin{aligned} u = v = w = t = 0 \quad &\text{at } \eta = 0 \\ u = v = w = t = \xi = 0 \quad &\text{at } \eta = \infty \\ u - u^0 = v = w = \xi = t = 0 \quad &\text{at } x = 0 \end{aligned} \tag{22}$$

For simplicity, the initial amplitude function u^0 is set uniform and the other velocity components u, v and w are set zero. However, the magnitudes of the velocities v and w will be generated in the next x steps. The magnitude of the initial amplitude function, $u^0 = 10^{-4}$ is used in the present study. In the experiment of Swearingen and Blackwelder [11], the free-stream turbulence level in their well-controlled wind tunnel was less than 0.07% that corresponding to the perturbation velocity u with magnitude between 10^{-4} and 10^{-3}.

Equations (17)–(21) and boundary conditions (Equations (7) and (15)) in the x–η plane are for unknown u, t, ξ, v, w, f and θ_b, with three fixed values of a, M, and $G_{L,\mathrm{rot}}$.

By giving a series value of a, the largest amplification of the perturbation quantities along the x direction determines the value of critical wave number a^*. One may prove analytically the homogeneity of L in Equations (17)–(21) by considering the dimensionless transformations (15), i.e. $v \sim L^{1/2}$, $w \sim L^{1/2}$, $a \sim L^{1/2}$, $x \sim L^{-1}$, $y \sim L^{-1/2}$, $z \sim L^{-1/2}$, and $\xi \sim L$ (variables of u, η, and f are independent of L). In the computation, the selection of $G_{L,\mathrm{rot}}$ does not change the local critical rotation number $G_{X,\mathrm{rot}}$ and the critical wave number $(a x^{1/2})^*$. This is also proved by using several values of $G_{L,\mathrm{rot}}$ in computation. In the present study, a fixed value $G_{L,\mathrm{rot}} = 500$ is used for demonstrating the results.

The local friction factor and the local Nusselt number of the basic and perturbed flows can also be expressed, respectively, as

$$C_{fX} = C_{\mathrm{fb}} + C_{\mathrm{fp}} = \frac{\tau_{\mathrm{wb}} + \tau_{\mathrm{wp}}}{\frac{1}{2}\rho U_\infty^2} = 2\,Re_X^{-1/2}\left[f''(0) + \left.\frac{\partial u}{\partial \eta}\right|_w\right] \tag{23}$$

$$Nu_X = Nu_{\mathrm{b}} + Nu_{\mathrm{p}} = \frac{(h_{\mathrm{b}} + h_{\mathrm{p}})X}{k} = -\,Re_X^{1/2}\left[\theta_{\mathrm{b}}'(0) + \left.\frac{\partial t}{\partial \eta}\right|_w\right] \tag{24}$$

where τ_{w} and h are the local wall shear stress and local heat transfer coefficient, respectively. The subscripts b and p indicate the basic and perturbed flows, and k is the fluid thermal conductivity. Note that the Nu_X is based on the thermal boundary condition of constant wall temperature.

NUMERICAL PROCEDURE

A finite difference scheme based on the weighting function [12] with second-order accuracy in both η and x is used. The step-by-step procedure is listed as follows.

(1) Assign Pr, Ro, M, and $Re_L^{1/2}$ to obtain the basic flow and temperature distribution. The value of Pr is 0.7 (air), $Ro = 1$, $Re_L^{1/2} = 250$ ($G_{L,\mathrm{rot}} = 500$) and $M = 0$–3 are used in the present study. Grids size of $\Delta x = 0.002$, $\Delta\eta = 0.02$, $\eta_\infty = 10$, and assigned x are used to perform the numerical experiment.

(2) Solve Equations (5) and (6) with boundary conditions (7) to obtain the quantities f_{b} and θ_{b}.
The basic flow quantities must meet the convergence criteria at the streamwise position.

$$\mathrm{Max}\left(\frac{|\Gamma_{i,j}^{(n+1)}| - |\Gamma_{i,j}^{(n)}|}{\Gamma_{i,j}^{(n+1)}}\right) \leqslant 10^{-5}$$

where Γ are the basic quantities f_{b} and θ_{b} of nodal point (i,j) at the nth number of iteration.

(3) Assign zero initial values of u, v, w, and ξ, initial velocity at the leading edge, $u^0 = 10^{-4}$ and various values of wave number a.

(4) Solve Equations (17), (18) and (19) for u, t and ξ distributions at the next x step. Values of ξ on boundary are evaluated with previous iteration data of v and w in the interior region.

(5) Solve Equations (20) and (21) for v and w with the obtained u and ξ.

(6) Repeat steps (3) and (4), until the perturbation quantities meet the convergence criteria at the streamwise position.

$$\mathrm{Max}\left(\frac{|\zeta_{i,j}^{(n+1)}| - |\zeta_{i,j}^{(n)}|}{\zeta_{i,j}^{(n+1)}}\right) \leqslant 10^{-5}$$

where $\zeta_{i,j}^{(n)}$ are the perturbation quantities u, v, w, t and ξ of nodal point (i,j) at the nth number of iteration.

(7) Calculate the local friction factor and Nusselt number of the vortex flow.

(8) Repeat steps (3)–(6) at the next mainstream position (x) until a desired mainstream position (x_{cr}) is reached.

The absolute values of perturbation quantities are growing along the mainstream direction. For each wave number a, the onset mainstream position is reached in the x localization where the criterion $\mathrm{Max}_j\,|u_{i,j}^{(n)}| = 0.01$ is satisfied. Various onset positions x_{cr} can be determined for different values of wave number a. The minimum x_{cr} denoted by x^* is the most probable onset position and the corresponding wave number is denoted by a^*. The local critical Goertler is $G_{X,\mathrm{rot}}^* = G_{L,\mathrm{rot}} \times x^{*3/2}$ and the local wave number is $a^* x^{*1/2}$ for this computation.

The criterion for determination of the onset of longitudinal vortices using the technique of velocity measurement in experiments can be explained as follows.

Hot-wire anemometry is employed for the measurement of axial velocity fluctuation along a direction normal to the longitudinal vortices. Typically, detectable velocity disturbance by hot-wire recording is around 0.001 m/s for free-stream velocity $U_\infty = 0.1$–1 m/s. Then the dimensionless axial perturbation velocity is around 0.01–0.001. Meanwhile, LDA is also employed for the measurement. Typically, the LDA recording in velocity disturbance is 0.0001 m/s for free-stream velocity $U_\infty = 0.1$–1 m/s. Then the dimensionless axial perturbation velocity is around 0.001–0.0001. By considering both velocity measurement techniques, it is reasonable to select $u = 0.01$ for the onset criterion for the longitudinal vortices. Then the longitudinal vortices can be observed for $\mathrm{Max}_j\,|u_{i,j}^{(n)}| = 0.01$ in the numerical solution by the velocity measurement techniques. Also, by comparison of the onset criterion between $\mathrm{Max}_j\,|u_{i,j}^{(n)}| = 0.01$ and 0.005 in the numerical experiment, the values of the onset position x^* increases less than 10%. It is reasonable to set in the numerical solution for the onset criterion of longitudinal vortices.

The grids tested for various Δx and $\Delta\eta$ are listed in Table I. A grid size of $\Delta x = 0.002$, $\Delta\eta = 0.02$ and $\eta_\infty = 10$ is used to perform the numerical experiment in the present study. To check the validity of the linear equations (17)–(21), the order of magnitude of nonlinear terms of perturbation equations near the onset position are checked. The calculated data are

Table I. Grid size test for $G_{L,\mathrm{rot}} = 500$, $a^* = 1.52$, $M = 0$, and $Pr = 0.7$.

Δx	$\Delta\eta$	$x = 0.1$	0.2	0.3	0.4	0.45
0.002	0.02	0.01671*	0.1033	1.613	6.600	57.51
0.002	0.01	0.01671	0.1033	1.611	6.558	57.50
0.001	0.02	0.01664	0.1031	1.610	6.557	57.48

*These are the maximum values of perturbation velocity $u/0.01$ at the specified x position.

substituted into the individual terms of the x-momentum equation. The orders of the nonlinear terms are two orders of magnitude smaller than the order of linearized inertia terms. Therefore, the linear theory is valid for the estimation of magnetic effect on the onset of longitudinal vortices in a laminar boundary layer flow with rotation.

RESULTS AND DISCUSSION

The typical development of the dimensionless perturbation amplitudes u, v, w, and t at $x = 0.3, 0.35$ and 0.4 for $Pr = 0.7$, $M = 0$, $Ro = 1$, $G_{L,\mathrm{rot}} = 500$, $a^* = 1.52$, and positive rotation (anticlockwise) is shown in Figure 2. The magnitude of v and w are larger than

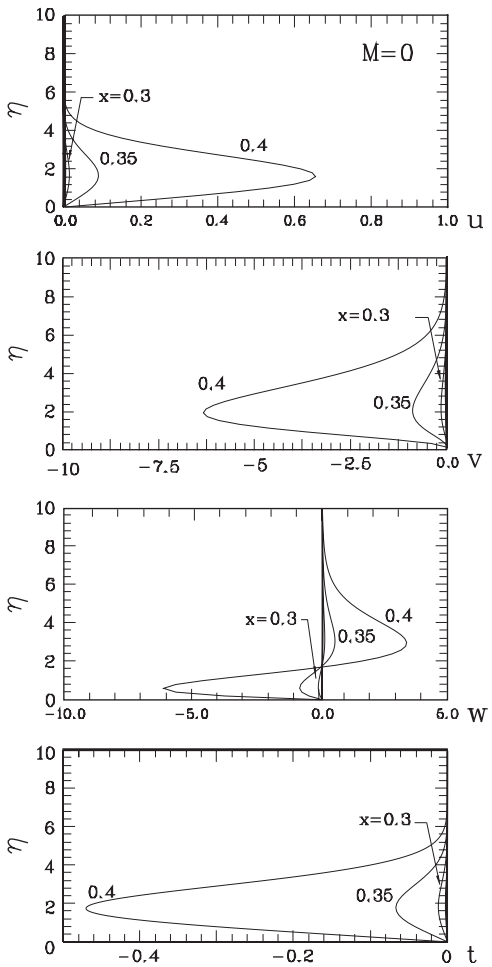

Figure 2. Development of perturbation amplitude profiles at specified x positions for positive rotation, $Pr = 0.7$, $Ro = 1$, $G_{L,\mathrm{rot}} = 500$, $a^* = 1.52$ and $M = 0$.

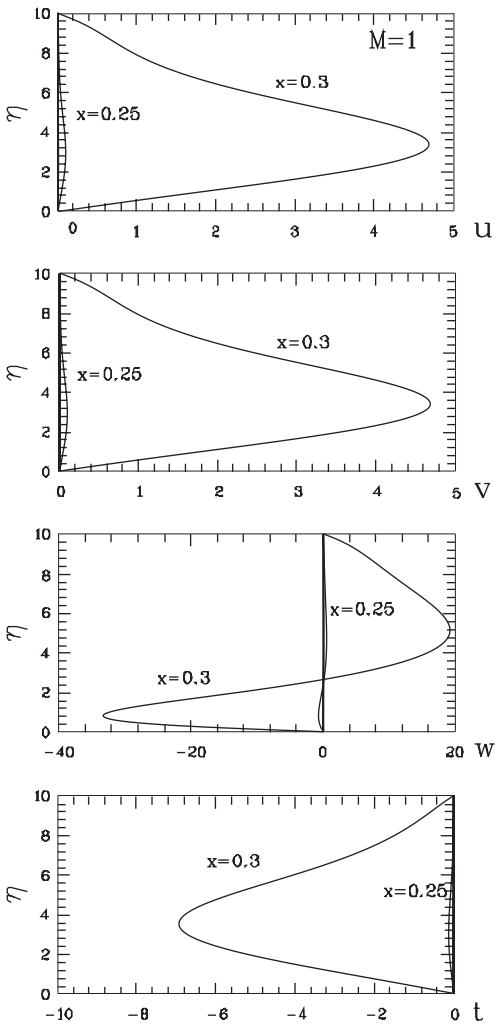

Figure 3. Development of perturbation amplitude profiles at specified x positions for positive rotation, $Pr = 0.7$, $Ro = 1$, $G_{L,\mathrm{rot}} = 500$, $a^* = 1.52$ and $M = 1$.

those of u and t because the scaling factor $Re_L^{-1/2}$ is included in these quantities. The shapes of the v and w profiles may be regarded as a vortex pattern. Figure 3 depicts the dimensionless perturbation amplitude functions at $x = 0.25$, and 0.3 with $M = 1$. It is seen that the values of perturbation amplitude functions are increased with the destabilizing effect of Lorentz force.

It is also interesting to study numerically the variations of friction factor and heat transfer coefficient after the onset of longitudinal vortices. The variations of local $C_{fX} = C_{\mathrm{fb}} + C_{\mathrm{fp}}$ and $Nu_X = Nu_{\mathrm{b}} + Nu_{\mathrm{p}}$ along axial direction at $z = 0$ with $M = 0, 1, 2$ are shown in Figures 4 and 5, respectively. The friction factor coefficient for the turbulent boundary layer flow based

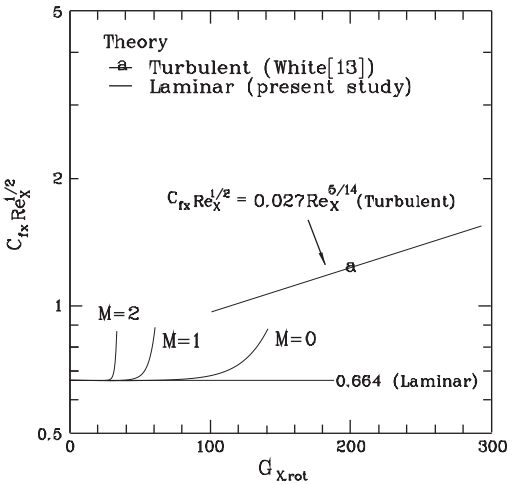

Figure 4. Local friction factor versus local Goertler number for $Pr = 0.7$, $Ro = 1$, and $Re_L^{1/2} = 250$.

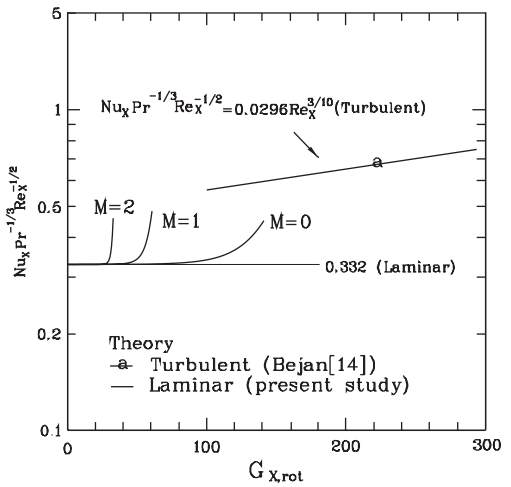

Figure 5. Local Nusselt number versus local Goertler number for $Pr = 0.7$, $Ro = 1$, and $Re_L^{1/2} = 250$.

on the one-seventh power law velocity profile with $M = 0$ (White [13]) is

$$C_{fX} \approx 0.027\, Re_X^{-1/7} \quad \text{or} \quad C_{fX}\, Re_X^{1/2} \approx 0.027\, Re_X^{5/14} = 0.027[(G_{X,\text{rot}}\, Re_L/2Ro)^{2/3}]^{5/14} \tag{25}$$

and the correlation equation for turbulent forced convection with $M = 0$ (Bejan [14]) is

$$Nu_X = 0.0296\, Re_X^{4/5}\, Pr^{1/3} \quad \text{or} \quad Nu_X\, Pr^{-1/3}\, Re_X^{-1/2} = 0.0296\, Re_X^{3/10}$$
$$= 0.0296[(G_{X,\text{rot}}\, Re_L/2Ro)^{2/3}]^{3/10} \tag{26}$$

In Figures 4 and 5, the friction factor and the Nusselt number for turbulence forced convection are shown only for comparison. The local friction factor and the local Nusselt number start to deviate from the laminar forced convection profile at downstream of x^*, due to the secondary longitudinal vortex flow on a positive rotating boundary layer. The magnetic field parameter has a destabilizing effect on the flow and the critical values of $G^*_{X,\mathrm{rot}}$ decreases with an increase in the magnetic field parameter.

The local critical values of Goertler number ($G^*_{X,\mathrm{rot}}$), and wave number ($a^*x^{*1/2}$) can be interpreted as follows: they may be converted to $G^*_{\delta,\mathrm{rot}}$ and $(a'\delta)^*$, respectively, by the following transformations:

$$G^*_{\delta,\mathrm{rot}} = \frac{U_\infty \delta}{\mu}\sqrt{\frac{\Omega\delta}{U_\infty}} = \left(\frac{1}{2}\times 5^3 \times G^*_{X,\mathrm{rot}}\right)^{1/2} \quad \text{and} \quad (a'\delta)^* = \left(\frac{2\pi}{\lambda}\frac{5X}{Re_X^{1/2}}\right)^* = 5(a^*x^{*1/2}) \qquad (27)$$

where δ represents the local boundary layer thickness, defined as $\delta = 5X/Re_X^{1/2}$.

Figure 6 summarizes the results of the present and previous works on the vortex instability in a rotating laminar boundary layer. It is seen in Figure 6 that there is a significant difference of one order of magnitude between experimental data and the previous theoretical prediction with $M = 0$ (Matubara and Masuda [13]). The values of critical $G^*_{\delta,\mathrm{rot}}$ with $M = 0$ of the present study (the curve line coincides with the results obtained by Lin and Hwang [6]) show good agreement with the previous experimental results (Matubara and Masuda [9] and Lin [15]). The experimental data of rotation number value $Ro = 0.87$–1.52 by Matubara and Masuda [9] and $Ro = 0.56$–1.12 by Lin [15] were employed. Thus, the corresponding data obtained with present methodology ($Ro = 1$) are comparable with the experimental results obtained by Matubara and Masuda [9] and Lin [15] (at the same order, i.e. $Ro \sim O(1)$). Wave instability was the primary instability mechanism for a Blasius flow over a flat plate. However, vortex instability was the primary instability mechanism for a Blasius boundary

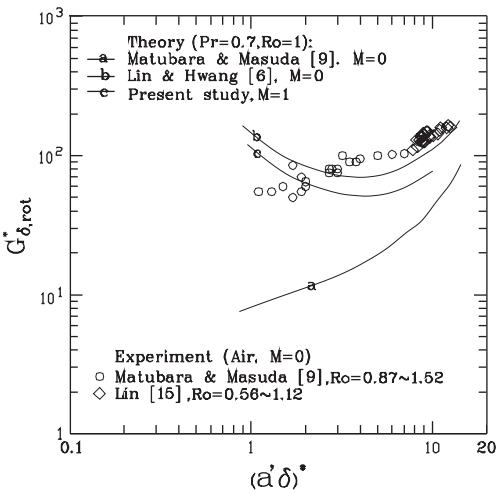

Figure 6. The relation between the critical values $G^*_{\delta,\mathrm{rot}}$ and wave number $(a'\delta)^*$.

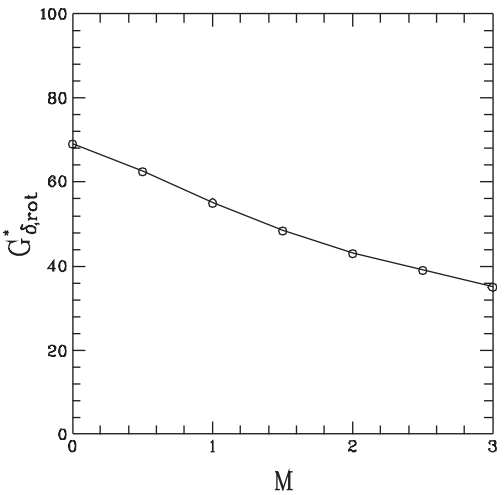

Figure 7. $G^*_{\delta,\mathrm{rot}}$ versus magnetic field parameter M for $Pr = 0.7$, $Ro = 1$, and $Re_L^{1/2} = 250$.

layer flow over a rotating flat plate, due to the effect of the Coriolis force, as stated in Reference Lin and Hwang [6]. The critical values of $G^*_{\delta,\mathrm{rot}}$ with $Ro = 1$ and $M = 1$ decreases approximately by 0.8 times the critical values of $G^*_{\delta,\mathrm{rot}}$ with $Ro = 1$ and $M = 0$, as shown in Figure 6. Vortex instability was the primary instability mechanism due to coupling effects of Lorentz force with the Coriolis force. One can concluded that the magnetic effect has found to be more destabilizing on the onset of longitudinal vortex of the flow.

The effect of magnetic field parameter M on the critical rotational Goertler number $G^*_{\delta,\mathrm{rot}}$ is shown in Figure 7. It can be observed from the data that an increase in the magnetic field parameter M decreases the value of critical rotational Goertler number $G^*_{\delta,\mathrm{rot}}$. An increase in the magnetic field parameter M from 0 to 3 decreases approximately two times the value of critical rotational Goertler number $G^*_{\delta,\mathrm{rot}}$ on a rotating flat plate. The flow is more unstable due to coupling effects of Lorentz force with the Coriolis force.

CONCLUSIONS

In this paper, a standard linear stability model was used to make a numerical study on the effect of a magnetic field on the formation of longitudinal vortices in a rotating laminar boundary layer. Besides others, the following conclusions were taken.

An increase in the magnetic field parameter M decreases the value of critical rotational Goertler number $G^*_{\delta,\mathrm{rot}}$. An increase in the magnetic field parameter M from 0 to 3 decreases by a factor of 2, the value of the critical rotational Goertler number $G^*_{\delta,\mathrm{rot}}$ on a rotating flat plate. The flow is more unstable due to coupling effects of Lorentz force with the Coriolis force. The results of this work show good agreement with the previous experimental results.

NOMENCLATURE

a'	dimensional wave number, $a' = 2\pi/\lambda$
a	dimensionless wave number, $a = a'L/Re_L^{1/2}$
B_0	uniform magnetic field strength (Wb/m^2)
C_f	local friction factor, $\tau_W/(\rho U_\infty^2/2)$
F	velocity, pressure or temperature function
f	reduced stream function, $\psi(\mu X U_\infty)^{-1/2}$
$G_{X,\mathrm{rot}}$	local rotational Goertler number, $G_{X,\mathrm{rot}} = 2(\Omega X/U_\infty)Re_X^{1/2}$
g	coefficient of gravity acceleration (m/s^2)
h	local heat transfer coefficient ($W\,m^{-2}\,K^{-1}$)
k	thermal conductivity (W/mK)
L	characteristic length or plate length (m)
M	magnetic field parameter, $M = \sigma B_0^2 L/\rho U_\infty$
p', p	dimensional and dimensionless pressure, $p' = \rho U_\infty^2 p/Re_L$
Pr	Prandtl number, μ/α
Nu_X	local Nusselt number, hX/k
Re_L	Reynolds number based on characteristic length, $U_\infty L/\mu$
Re_X	local Reynolds number, $U_\infty X/\mu$
Ro	rotation number based on characteristic length, $\Omega L/U_\infty$
T	temperature (K)
t', t	dimensional and dimensionless perturbation temperature, $t' = (T_w - T_\infty)t$
u^0	initial constant perturbation velocity at $x = 0$
U, V, W	dimensional velocity components (m/s)
u, v, w	dimensionless perturbation velocity components
u', v', w'	perturbation velocity components (m/s)
X, Y, Z	Cartesian coordinates (m)
x, y, z	dimensionless Cartesian coordinates

Greek letters

α	thermal diffusivity of fluid (m^2/s)
β	coefficient of thermal expansion (1/K)
δ	boundary layer thickness (m)
η	Blasius similarity variable, $Y/(\mu X/U_\infty)^{1/2}$
θ_b	dimensionless basic temperature $(T - T_\infty)/(T_w - T_\infty)$
λ	wave length in Z direction (m)
μ	kinematic viscosity of fluid (m^2/s)
ξ	vorticity function in X direction (1/s)
ρ	density of fluid (kg/m^3)
σ	electrical conductivity, mho
τ_w	local wall shear stress
ψ	stream function (m^2/s)
Ω	angular speed (rad/s), defined positive for anticlockwise rotation

Superscript

*	onset position

Subscripts

b	basic flow quantity
p	perturbation quantity
w	wall condition
X	local coordinate
∞	free stream condition
L	characteristic length or plate length

ACKNOWLEDGEMENTS

The author would like to acknowledge the National Science Council for its support of the present work through project NSC 93-2212-E-233-002. Meanwhile, the author appreciates the reviewers who have given valuable comments to improve the quality of this paper.

REFERENCES

1. Conrad PW. The effects of rotation on the stability of laminar boundary layers on curved walls. *Report FLD-9*, Mechanical Engineering Department, Princeton University, 1962.
2. Chawla M. The stability of boundary layer flow subject to rotation. *Ph.D. Thesis*, Michigan State University, 1962.
3. Koyama H, Masuda S, Ariga I, Watanabe I. Stabilizing and destabilizing effects of coriolis force on two-dimensional laminar and turbulent boundary layers. *ASME Journal of Engineering for Power* 1979; **101**: 23–31.
4. Masuda S, Okamae K, Agiga I. Transition of boundary layer on rotating flat plate. *Proceedings of the IUTAM Symposium on Laminar-Turbulent Transition*, Novosibirsk, USSR, 1984; 699–704.
5. Masuda S, Matubara M. Visual study of boundary layer transition on rotating flat plate. *3rd IUTAM Symposium on Laminar-Turbulent Transition*, Toulouse, France, 1989; 699–704.
6. Lin MH, Hwang GJ. Numerical study of the formation of longitudinal vortices in laminar boundary layers with rotation. *Journal of the Chinese Society of Mechanical Engineers* 2000; **21**:341–349.
7. Hwang GJ, Lin MH. Estimation of the onset of longitudinal vortices in a laminar boundary layer heated from below. *ASME Journal of Heat Transfer* 1995; **117**:835–842.
8. Singh AK, Chandran P, Sacheti NC. Effect of transverse magnetic field on a flat plate thermoter. *International Journal of Heat and Mass Transfer* 2000; **43**:3253–3257.
9. Matubara M, Masuda S. Three-dimensional instability in rotating boundary layer. *Boundary Layer Stability and Transition to Turbulence* (ASME), FED-vol. 114, 1991; 103–107.
10. Chen CT, Lin MH. Effect of rotation on Goertler vortices in the boundary layer flow on a curved surface. *International Journal for Numerical Methods in Fluids* 2002; **40**:1327–1346.
11. Swearingen JD, Blackwelder RF. The growth and breakdown of streamwise vortices in the presence of a wall. *Journal of Fluid Mechanics* 1987; **182**:255–290.
12. Lee SL. Weighting function scheme and its application on multidimensional conservation equations. *International Journal of Heat and Mass Transfer* 1989; **32**:2065–2073.
13. White FM. *Viscous Fluid Flow* (2nd edn). McGraw-Hill: New York, 1991; 378.
14. Bejan A. *Heat Transfer* (1st edn). Wiley: New York, 1993; 260.
15. Lin CH. Visualization of vortex instability in radically rotating rectangular channel. *Master Thesis*, National Tsing-Hwa University, Taiwan, 1996.

